Manufacturing of thermally stable nanocrystalline aluminum alloys and studying their corrosion behavior in Arabian Gulf seawater

El-Sayed M. Sherif [*], Hany Rizk Ammar[**], Khalil Abdelrazek Khalil[***]

[*]Center of Excellence for Research in Engineering Materials (CEREM), Advanced Manufacturing Institute, King Saud University, P. O. Box 800, Al-Riyadh 11421, Saudi Arabia, esherif@ksu.edu.sa
[**]Metallurgical and Materials Engineering Department, Faculty of Petroleum and Mining Engineering, Suez University, Suez, Egypt, Hany_Ammar@uqac.ca
[***]Mechanical Engineering Department, College of Engineering, King Saud University, P.O. Box 800, Al-Riyadh 11421, Saudi Arabia, kabdelmawgoud@ksu.edu.sa
[*]Corresponding author: Tel. 00966114670760; Fax. 00966114670199

ABSTRACT

The as-received metal powders were used to synthesis bulk nanocrystalline Al; Al-10%Cu; and Al-10%Cu-5%Ti alloys using mechanical alloying and high frequency induction heat sintering. The corrosion of these materials in natural Arabian Gulf seawater (AGS) has been investigated using different electrochemical and spectroscopic techniques. The impedance spectroscopy measurements showed that the presence of Cu decreases the corrosion of Al and that effect was further reduced when adding Ti. Polarization experiments confirmed that adding Cu and Ti decreases the corrosion parameters for Al in AGS. Current vs.time at constant potential data indicated that Al suffers both uniform and pitting corrosion, which decrease in the presence of Cu and Ti. The surfance investigations confirmed the decrease of deterioration for Al surface containing Cu and Ti. All measurements were consistent with each other and indicated clearly that the corrosion resistance of these materials in AGS increases in the order Al-10% Cu-5% Ti > Al-10% Cu > Al.

Keywords: aluminum alloys, corrosion, mechanical alloying, seawater

1 INTRODUCTION

Aluminum and its alloys have been widely used as a material in the fields of transport, building, containers, household appliances, electrical engineering, aircraft and aerospace, etc due to its many good characteristics [1,2]. The high resistance of Al and its alloys against corrosion comes from the ability of these maerials in developing a compact, adherent, and continuous oxide film on their surfaces upon exposure to the atmosphere or aqueous solutions [3-7]. Even though, the formation of aluminum oxide film does not have the ability to protect the surface in corrosive media such as natural seawater and solutions containing high chloride concentrations where, aluminum suffers both uniform and pitting corrosion [8-11].

Mechanical Alloying (MA) is a solid-state powder processing method that requires a repeated welding, fracturing, and re-welding of powder particles in ball mill. MA can be used to synthesize variety of equilibrium and non-equilibrium alloy phases from elemental powders. The use of MA technique in materials production presents several advantages that include refining of the grain sizes to the nanoscale, producing new phases, production of fine dispersoid of second phase particles, extending the equilibrium solid solubility limit, and alloying of immiscible alloying elements [12-16]. There are several factors that influence the properties of the processed products and make it unique using MA technique. Therefore, the MA method has been used in developing several alloys including aluminum ones; some of these are Al-Mg, Al-Ti, Al-Fe, and Al-Zr alloys [17-22].

The present study aimed at developing thermally stable nanocrystalline pure aluminum and two of its alloys, namely Al-10%Cu and Al-10%Cu-5%Ti by using MA technique. The aim was also extended to study the corrosion behavior of these nanocrystalline materials in Arabian Gulf seawater by employing a variety of electrochemical and spectroscopic techniques. The electrochemical methods included the use of the electrochemical impedance spectroscopy, potentiodynamic polarization, and chronoamperometric current-time at constant potential. Spectroscopic investigations were carried out using scanning electron microscopy and energy dispersive X-ray analyzer.

2 EXPERIMENTAL PROCEDURES

2. 1 Manufacturing of Al and its Alloys

Metal powders of high purity Al, Cu, and Ti having an average particles size of 100 microns were used as received to synthesis nanocrystalline Al, Al-10%Cu, and Al-10%Cu-5%Ti alloys using MA method. In order to prevent the powders agglomeration, stearic acid with 5 wt.% was used as a process control agent and also to maintain the balance between cold welding and fracturing of powder particles.

Two milling times of 3 and 6 hours and two ball-to-powders weight ratio (BPR) of 30:1 and 90:1 were applied to establish the conditions for getting the nanocrystalline structure for the obtained materials. The mechanical alloying process was carried out using 1S-attritor. The milling process was undertaken under argon atmosphere to avoid any contamination of the processed powders from the atmosphere.

Powder consolidation was carried out using a high frequency induction heat sintering (HFIHS) machine. The sintering conditions applied in this process were heating rate of 350 °C/min; sintering time of 4 minutes; sintering temperature of 400°C; applied pressure of 750 Kgf/cm^2 (100 MPa); cooling rate of 400°C/min and the process was carried under vacuum of 10^{-3} Torr. The processed powders were placed in a graphite die of 45 mm diameter and then introduced into the HFIHS.

The crystallite size of the produced materials was determined by XRD data and Scherrer equation. The microstructure of these materials was determined by using a field emission gun scanning electron microscope.

2. 2 Corrosion Measurements

The Arabian Gulf seawater was obtained from the eastern region of the Arabian Gulf (eastern coast, Jubail, Dammam, Kingdom of Saudi Arabia). A conventional electrochemical cell with a three-electrode configuration was used; a platinum foil and an Ag/AgCl electrode (in the saturated KCl) were used as the counter and reference electrodes, respectively. The fabricated nanocrystalline Al, Al-10%Cu, and Al-10%Cu-5%Ti rods were used as the working electrode. Before measurements, the face of the working electrode to be immersed in the AGS, was first ground successively with metallographic emery paper of increasing fineness up to 1000 grit then cleaned using doubly-distilled water, degreased with acetone, washed using doubly-distilled water again and finally dried with dry air.

An Autolab Potentiostat (PGSTAT20 computer controlled) operated by the general purpose electrochemical software (GPES) version 4.9 was used to perform the electrochemical experiments. Potentiodynamic polarization measurements were obtained by scanning the potential in the forward direction from -1.7 to -0.25 V vs. Ag/AgCl at a scan rate of 0.001V/s. Chronoamperometric current-time experiments were carried out by stepping the potential of the aluminum samples at – 0.5 V for 30 min. The electrochemical impedance spectroscopy (EIS) tests were caried out at the open-circuit potential (E_{OCP}) over a frequency range of 100 kHz – 100 mHz, with an ac wave of ± 5 mV peak-to-peak overlaid on a dc bias potential, and the impedance data were collected using Powersine software at a rate of 10 points per decade change in frequency. All measurements were obtained at room temperature and after 1 h immersion of the working electrode in AGS.

The scanning electron microscopy (SEM) images and the energy dispersive X-ray (EDX) analyses were obtained from the surface of Al, Al-10%Cu and Al-10%Cu-5%Ti after their immersions in the AGSW for 1 h before applying and amount of -0.50 V vs. Ag/AgCl on the surfaces of the electrodes for another 1 h. The SEM/EDX data were collected by using a JEOL model JSM-6610LV (Japanese made) scanning electron microscope with an energy dispersive X-ray analyzer attached.

3 RESULTS AND DISCUSSION

3. 1 Potentiodynamic Polarization (PP)

Fig. 1 shows the PP curves obtained for (a) Al, (b) Al-10%Cu and (c) Al-10%Cu-5%Ti, respectively. It is well known that the cathodic reaction for Al in near neutral solutions is the oxygen reduction as follows [3,4];

$$O_2 + 2H_2O + 4e^- = 4OH^- \quad (1)$$

While, the anodic reaction is the dissolution of aluminum due to the increase of current by increase of potential [4];

$$Al = Al^{3+} + 3e^- \quad (2)$$

After the rapid increases of current, the polarization curve shows a large passivation region, which is most probably due to the formation of an oxide film and/or a corrosion product layer on the surface of Al and its alloys as follows:

$$Al^{3+} + 3\ OH^- = Al(OH)_{3,ads} + 3\ e^- \quad (3)$$

The $Al(OH)_{3,ads}$ transforms to aluminum oxide;

$$Al(OH)_{3,ads} = Al_2O_3 + H_2O \quad (4)$$

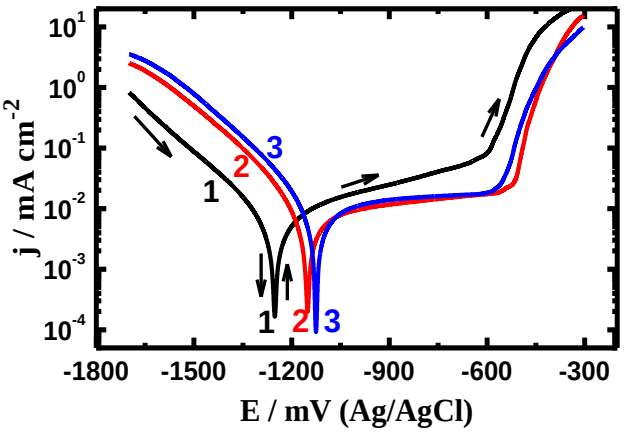

Figure 1. Potentiodynamic polarization curves obtained for (1) Al, (2) Al-10%Cu, and (3) Al-10%Cu-5%Ti, respectively after 1 h immersion AGS.

The formation of Al_2O_3 (Eq. 4) protects the surface against corrosion until the potential reaches the breakdown value. This is indicated by abrupt increase of current as a result of the breakdown of the passive layer and the occurrence of pitting corrosion [3,4]. The breakdown of the passive oxide film also allows aluminum surface to be

attacked by the aggressive ions presented in the solution, i.e. chlorides, to form aluminum chloride complex, $AlCl_4^-$, as can be expressed by the following reaction;

$$Al^{3+} + 4\ Cl^- = AlCl_4^- \qquad (5)$$

The formation of $AlCl_4^-$ leads to the occurrence of pitting corrosion.

It is also seen from Fig. 1 that the presence of 10% Cu as alloying element with the nanocrystalline Al decreased the values of anodic current, corrosion current, and passivation current as well as shifted the values of corrosion potential towards the less negative direction. The presence of 5% Ti to the Al-10%Cu alloy produced further passivation.

3. 2 Current-time Measurements

Fig. 2 shows the current-time curves obtained for (1) Al, (2) Al-10%Cu and (3) Al-10%Cu-5%Ti, respectively after their immersion in AGS before applying a potential of -0.50 V vs. Ag/AgCl for 30 min. It is seen from Fig. 2 (curve 1) that the current abruptly increased in the first few moments of the measurement due to the dissolution of an aluminum oxide (Al_2O_3) film. The current of Al started to decrease with the appearance of some of its fluctuations after about 10 min, as a result of the occurrence of pitting corrosion.

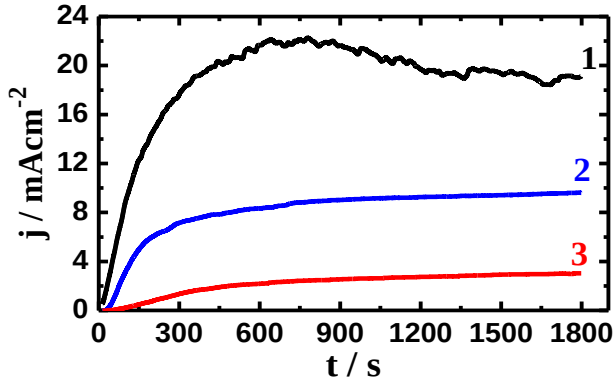

Figure 2. Current-time curves obtained for (1) Al, (2) Al-10%Cu and (3) Al-10%Cu-5%Ti, respectively after their immersion in AGS for 1 h then apply a potential of -0.5 V.

The addition of 10%Cu and further 5%Ti led to decreasing the rapid increases in the current and its absolute values as well as the disappearance of its fluctuations for the alloys compared to the currents recorded with the pure aluminum electrode. This behavior this confirms that the nanocrystalline Al suffers the highest rate of uniform corrosion and pitting attack. While, the addition of Cu and Ti passivated Al and their corrosion decreased in the order Al > Al-10%Cu > Al-10%Cu-5%Ti.

3. 3 EIS Measurements

The EIS technique has been widely employed in understanding the mechanism of corrosion and passivation processes for metallic materials in harsh media [23-27]. The Nyquist plots obtained for (1) Al, (2) Al-10%Cu, and (3) Al-10%Cu-5%Ti, respectively after 1 h immersion in AGS are shown in Fig. 3. These plots were best fitted to the equivalent circuit model shown in Fig. 4; the values of the symbol parameters obtained by fitting to this equivalent circuit are listed in Table 1. The symbols of the elements of the equivalent circuit are defined according to usual convention. Where, R_S is the solution resistance, Q_1 and Q_2 represent the constant phase elements (CPEs), Rp_1 is the polarization resistance for the interface between the Al and Al alloys surface and a layer of corrosion product may be formed during the immersion in AGS and can be defined also as the chare transfer resistance, and Rp_2 is the plarization resistance between the corrosion product layer and the solution of AGS.

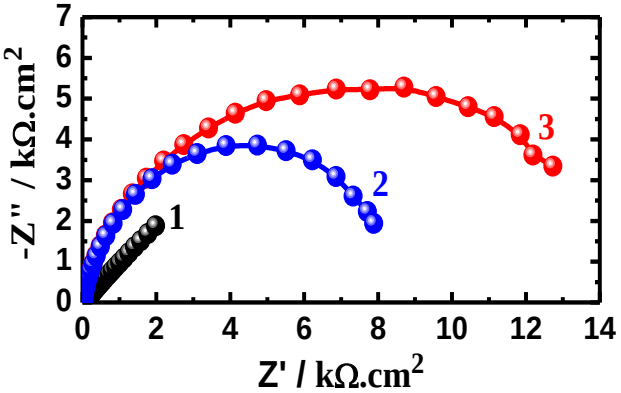

Figure 3. Nyquist plots obtained for (1) Al, (2) Al-10%Cu, and (3) Al-10%Cu-5%Ti after 1 h immersion in AGS.

It is seen from Fig. 3 that all plots showed only one semicircle and that the pure Al spectrum recorded the smallest diameter. The presence of 10%Cu with Al (curve 2) remarkably increased the diameter of the semicircle and further increment in the diameter was obtained in the presence of 10%Cu + 5%Ti (curve 3). This is due to the increased passivity of Al by the addition of Cu and further by the addition of Ti. This was further confirmed by the values of parameters listed in Table 1, where the values of R_S, Rp_1 and Rp_2 increased in the presence of Cu and further in the presence of Ti. The constant phase elements (CPEs, Q_1) represent double layer capacitors with some pores, On the other hand, Q_2 with its n value is between 0.5 and 0.54, represents Warburg impedance (W) that confirms the passivity of the surface of Al alloys in AGS, it does not take place via mass transfer.

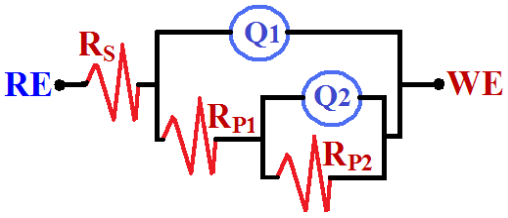

Figure 4. Equivalent circuit model used to fit EIS data.

Table 1. Parameters obtained by fitting the Nyquist plots shown in Fig. 3 with the equivalent circuit shown in Fig. 4.

Sample	EIS Parameter						
	R_S/ Ω cm^2	Q_1		R_{P1}/ kΩ cm^2	Q_2		R_{P2}/ kΩ cm^2
		Y_{Q1}/μ F cm^{-2}	n		Y_{Q2}/μ F cm^{-2}	n	
Al	8.8	2.22	0.8	1.24	2.3	0.5	1.76
Al-Cu	9. 7	1.396	0.9	7.5	1.7	0.6	3.28
Al-Cu-Ti	11.4	0.943	0.9	8.62	0.41	0.5	5.61

4 CONCLUSIONS

The present work reported the manufacturing of nanocrystalline Al, Al-10%Cu and Al-10%Cu-5%Ti using the mechanical alloying technique. The corrosion behavior of the fabricated materials in AGS was also reported using potentiodynamic polarization, chronoamperometric current-time and electrochemical impedance spctroscopy measurements. All measurements indicated that the nanocrystalline Al suffers both uniform and pitting corrosion in AGS medium. This because Al recorded the highest corrosion density, the most negative corrosion potential and the highest absolute current with increasing time at -0.5 V vs. Ag/AgCl. The addition of 10%Cu remarkably decreased the corrosion of Al through decreasing the corrosion current density, the aboslute current, and shifting the corrosion potential towards the less negative values. The presence of 5%Ti with the Al-Cu alloy further reduced the corrosion parameters and proved that the Al-10%Cu-5%Ti alloy has the best performance amongest all tested Al and Al-10%Cu at the same condition. Results together were in good agreement and confirmed clearly that the presence of 10%Cu enhances the corrosion resistance of Al and the presence of 5%Ti within the Al-10% Cu adds further passivation and the corrosion decreases in the order Al > Al-10%Cu > Al-10%Cu-5%Ti.

ACKNOWLEDGEMENTS

This project was supported by NSTIP strategic technologies program number (11-ADV1853-02) in the Kingdom of Saudi Arabia.

REFERENCES

[1] F. H. Latief, El-Sayed M. Sherif, A. A. Almajid and H. Junaedi, Journal of Analytical and Applied Pyrolysis, 92, 485-492, 2011.
[2] El-Sayed M. Sherif, Mahmoud S. Soliman, E. A. El-Danaf and A. A. Almajid, International Journal of Electrochemical Science, 8, 1103-1116, 2013.
[3] E. M. Sherif, S.-M. Park, Journal of the Electrochemical Society, 152, B205-B211, 2005.
[4] E. M. Sherif, S.-M. Park, Electrochimica Acta, 51, 1313-1321, 2006.
[5] K. F. Khaled, Corrosion Science, 52, 2905-2916, 2010.
[6] El-Sayed M. Sherif, E. A. El-Danaf, M. S. Soliman, A. A. Almajid, International Journal of Electrochemical Science, 7, 2846-2859, 2012.
[7] Serpil Şafak, Berrin Duran, Aysel Yurt, Gülşen Türkoğlu, Corrosion Science, 54, 251-259, 2012.
[8] El-Sayed M. Sherif, A. A. Almajid, F. H. Latif and H. Junaedi, International Journal of Electrochemical Science, 6, 1085-1099, 2011.
[9] G. Y. Elewady, I. A. El-Said and A. S. Fouda, International Journal of Electrochemical Science, 3, 177-190, 2008.
[10] T. Choh and T. Oki, Material Science and Technology, 3, 378-385, 1987.
[11] F. H. Latief, El-Sayed M. Sherif, Journal of Industrial and Engineering Chemistry, 18, 2129–2134, 2012.
[12] M. A. Shaikh, M. Iqbal, J. I. Akhter, M. Ahmad, Q. Zaman, M. Akhtar, M. J. Moughal, Z. Ahmed, and M. Farooque, Materials Letters, 57, 3681-3685, 2003.
[13] H. D. K. H. Bhadeshia, Materials Science and Technology, 16, 1404-1411, 2000.
[14] C. C. Koch, Materials Science and Engineering: A, 244, 39-48, 1998.
[15] C. C. Koch and J. D. Whittenberger, Intermetallics, 4, 339-355, 1996.
[16] E. Ma and M. Atzmon, Materials Chemistry and Physics, 39, 249-267, 1995.
[17] C. Suryanarayana, Progress in Materials Science, 46, 1-184, 2001.
[18] M. Krasnowski and T. Kulik, Materials Chemistry and Physics, 116, 631-637, 2009.
[19] T. T. Sasaki, T. Ohkubo and K. Hono, Acta Materialia, 57, 3529-3538, 2009.
[20] T.T. Sasaki, T. Mukai and K. Hono, *Scripta Materialia*, 57, 189-192, 2007.
[21] R. Lerf and D. G. Morris, Materials Science and Engineering: A, 128, 119-127, 1990.
[22] L. Shaw, H. Luo, J. Villegas and D. Miracle, Acta Materialia, 51, 2647–2663, 2003.
[23] W. Gao, Si Cao, Y. Yang, H. Wang, Jin Li and Y. Jiang, Thin Solid Films, 520, 6916-6921, 2012.
[24] V. Shinde, P. P. Patil, Materials Science and Engineering: B, 168,142-150, 2010.
[25] K. Darowicki, S. Krakowiak, P. Ślepski, Electrochimica Acta, 49, 2909-2918, 2004.
[26] P. Papakonstantinou, J. F. Zhao, A. Richardot, E. T. McAdams and J. A. McLaughlin, Diamond and Related Materials, 11, 1124-1129, 2002.
[27] F. L. Floyd, S. Avudaiappan, J. Gibson, B. Mehta and P. Smith, Progress in Organic Coatings, 66, 8-34, 2009.